Inorg. Chem. **2008**, *47*, 1134–1144

Employment of 2,6-Diacetylpyridine Dioxime as a New Route to High Nuclearity Metal Clusters: Mn_6 and Mn_8 Complexes

Theocharis C. Stamatatos,[†] Brian S. Luisi,[‡] Brian Moulton,[‡] and George Christou*[,†]

Departments of Chemistry, University of Florida, Gainesville, Florida 32611, and Brown University, Providence, Rhode Island 02912

Received October 12, 2007

The employment of the anion of 2,6-diacetylpyridine dioxime (dapdoH_2) as a pentadentate chelate in transition metal cluster chemistry is reported. The syntheses, crystal structures, and magnetochemical characterization are described for $[Mn_6O_2(OMe)_2(dapdo)_2(dapdoH)_4](ClO_4)_2$ (**1**), $[Mn_6O_2(OMe)_2(dapdo)_2(dapdoH)_4][Ca(NO_3)_4]$ (**2**), and $[Mn_8O_4(OH)_4(OMe)_2(N_3)_2(dapdo)_2(dapdoH)_2(H_2O)_2]$ (**3**). The reaction of $[Mn_3O(O_2CMe)_6(py)_3](ClO_4)$ with 3 equiv of dapdoH_2 (with or without 2 equiv of NEt_3) in MeOH gave **1**. The same cation, but with a $[Ca(NO_3)_4]^{2-}$ anion, was found in complex **2**, which was obtained from the reaction in MeOH between $Mn(NO_3)_2$, $Ca(NO_3)_2$, and dapdoH_2 in the presence of NEt_3. In contrast, addition of NaN_3 to several reactions comprising $MnCl_2$, dapdoH_2, and NEt_3 in MeOH gave the octanuclear complex **3**. Complexes **1**–**3** all possess rare topologies and are mixed-valence: $2Mn^{II}$, $4Mn^{III}$ for **1** and **2**, and $2Mn^{II}$, $6Mn^{III}$ for **3**. The core of the cation of **1** and **2** consists of two edge-sharing Mn_4 tetrahedra at the center of each of which is a μ_4-O^{2-} ion. Peripheral ligation is provided by two μ-OMe^-, four μ-dapdoH^-, and two μ_3-dapdo^{2-} groups. The core of **3** consists of two $[Mn^{II}Mn^{III}{}_3(\mu_3\text{-}O)_2]^{7+}$ "butterfly" units linked together by one of the μ_3-O^{2-} ions, which thus becomes μ_4. Peripheral ligation is provided by four μ-OMe^-, two μ-OH^-, two μ-dapdoH^-, and two μ_4-dapdo^{2-} groups. Variable-temperature, solid-state dc and ac magnetization studies were carried out on complexes **1**–**3** in the 5.0–300 K range; the data for **1** and **2** are identical. Fitting of the obtained magnetization versus field (*H*) and temperature (*T*) data by matrix diagonalization and including only axial anisotropy (zero-field splitting, *D*) established that **1** possesses an $S = 5$ ground state with $D = -0.24$ cm^{-1}. For **3**, low-lying excited states precluded obtaining a good fit from the magnetization data, and the ground state was instead determined from the ac data, which indicated an $S = 1$ ground state for **3**. The combined work demonstrates the ligating flexibility of pyridyl-dioxime chelates and their usefulness in the synthesis of new polynuclear Mn_x clusters without requiring the co-presence of carboxylate ligands.

Introduction

There continues to be an intense interest by many groups around the world in the synthesis and study of polynuclear 3d transition metal complexes, not least for their intrinsic architectural beauty and aesthetically pleasing structures.[1] Other reasons for this interest are varied. For manganese chemistry, for example, this interest derives from their relevance to two fields. First, the ability of Mn to exist in a number of oxidation states (II−IV) under normal conditions has resulted in this metal being at the active sites of several redox enzymes, the most important of which is the water-oxidizing complex (WOC) on the donor side of photosystem II in green plants and cyanobacteria.[2] The WOC comprises a tetranuclear Mn cluster, whose exact structure is still unclear, and is responsible for the light-driven, oxidative coupling of two molecules of water into dioxygen.[3,4] In addition, one Ca plays a crucial role in the oxygen-evolving complex (OEC) activity; without Ca, the OEC does not advance to the S_3 state.[5] Although there is considerable uncertainty about the Mn_4Ca structure obtained from crystal-

* Author to whom correspondence should be addressed. E-mail: christou@chem.ufl.edu.
† University of Florida.
‡ Brown University.

(1) Wang, X. J.; Langetepe, T.; Persau, C.; Kang, B.-S.; Sheldrick, G. M.; Fenske, D. *Angew. Chem., Int. Ed.* **2002**, *41*, 3818.

(2) (a) Ferreira, K. N.; Iverson, T. M.; Maghlaoui, K.; Barber, J; Iwata, S. *Science* **2004**, *303*, 1831. (b) Carrell, T. G.; Tyryshkin, A. M.; Dismukes, G. C. *J. Biol. Inorg. Chem.* **2002**, *7*, 2. (c) Cinco, R. M.; Rompel, A.; Visser, H.; Aromi, G.; Christou, G.; Sauer, K.; Klein, M. P.; Yachandra, V. K. *Inorg. Chem.* **1999**, *38*, 5988. (d) Yachandra, V. K.; Sauer, K.; Klein, M. P. *Chem. Rev.* **1996**, *96*, 2927.

10.1021/ic7020269 CCC: $40.75
Published on Web 01/04/2008

lography due to the current resolution,[6] there is little doubt that the OEC is indeed a heterometallic $[Mn_4CaO_x]$ cluster on the basis of other spectroscopic studies (i.e., XRD[2a,5b] and EXAFS[7]). Second, polynuclear Mn compounds containing Mn^{III} have been found to often have large, and sometimes abnormally large, ground-state spin values (S), which combined with a large and negative magnetoanisotropy have led to some of these species being able to function as single-molecule magnets (SMMs).[8] These are individual molecules that behave as magnets below a certain ("blocking") temperature.[9] Thus, they represent a molecular, "bottom-up" approach to nanomagnetism.[10]

As a result of the above, we have explored and successfully developed many new routes for the synthesis of polynuclear Mn complexes,[10,11] with nuclearities currently up to 84.[12] These procedures have included comproportionation reactions of simple starting materials,[13] aggregation of clusters of smaller nuclearity,[14] fragmentation of higher nuclearity clusters,[15] reductive aggregation or fragmentation of preformed clusters,[16] and electrochemical oxidation,[17] disproportionation,[18] or ligand substitution of preformed species,[14b,19] among others. As part of this work, we have also explored a wide variety of potentially chelating and/or bridging ligands that might foster formation of high nuclearity products. One

Scheme 1

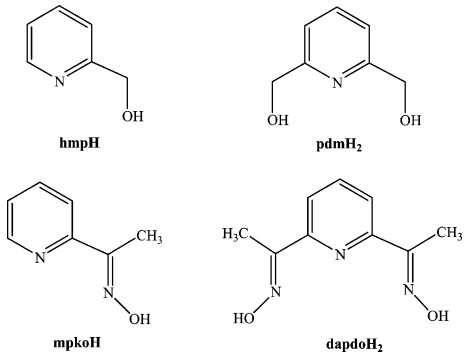

such family is the pyridyl alcohols, which have proven to be extremely versatile N,O_x ($x = 1$, hmpH; $x = 2$, $pdmH_2$; Scheme 1) chelating and bridging groups that have yielded a number of 3d metal clusters with various structural motifs, large S values, and SMM behaviors.[20,11b,21] More recently, we have been investigating a number of other N- and O-based chelates, and one of these has been the 2-pyridyl oximes, particularly methyl-2-pyridyl ketone oxime (mpkoH; Scheme 1). We recently reported, for example, the employment of mpkoH in Mn carboxylate chemistry, which gave the initial examples of triangular Mn^{III} SMMs by switching the exchange coupling from the more usual antiferromagnetic to ferromagnetic.[22] As an extension to this work with mpkoH, we have now asked what kind of products might result from the addition of another ketone oxime arm onto the mpkoH group but on the other side of the pyridine ring, much like the way that $pdmH_2$ is hmpH with another hydroxymethyl

(3) Law, N. A.; Caudle, M. T.; Pecoraro, V. L. In *Advances in Inorganic Chemistry*; Sykes, A. G., Ed.; Academic Press: London, 1998; Vol. 46, p 305.
(4) Yocum, C. F.; Pecoraro, V. L. *Curr. Opin. Chem. Biol.* **1999**, *3*, 182.
(5) (a) Cinco, R. M.; Holman, K. L. M.; Robblee, J. H.; Yano, J.; Pizarro, E.; Bellacchio, E.; Sauer, K.; Yachandra, V. K. *Biochemistry* **2002**, *41*, 12928. (b) Loll, B.; Kern, J.; Saenger, W.; Zouni, A.; Biesiadka, J. *Nature* **2005**, *438*, 1040.
(6) Dau, H.; Liebisch, P.; Haumann, M. *Phys. Chem. Chem. Phys.* **2004**, *6*, 4781.
(7) Yano, J.; Kern, J.; Sauer, K.; Latimer, M. J.; Pushkar, Y.; Biesiadka, J.; Loll, B.; Saenger, W.; Messinger, J.; Zouni, A.; Yachandra, V. K. *Science* **2006**, *314*, 821 and references therein.
(8) Christou, G.; Gatteschi, D.; Hendrickson, D. N.; Sessoli, R. *MRS Bull.* **2000**, *25*, 66.
(9) (a) Bircher, R.; Chaboussant, G.; Dobe, D.; Güdel, H. U.; Oshsenbein, S. T.; Sieber, A.; Waldmann, O. *Adv. Funct. Mater.* **2006**, *16*, 209. (b) Gatteschi, D.; Sessoli, R. *Angew. Chem., Int. Ed.* **2003**, *42*, 268. (c) Aubin, S. M. J.; Gilley, N. R.; Pardi, L.; Krzystek, J.; Wemple, M. W.; Brunel, L.-C.; Maple, M. B.; Christou, G.; Hendrickson, D. N. *J. Am. Chem. Soc.* **1998**, *120*, 4991. (d) Oshio, H.; Nakano, M. *Chem. Eur. J.* **2005**, *11*, 5178.
(10) Christou, G. *Polyhedron*, **2005**, *24*, 2065 and references therein.
(11) (a) Soler, M.; Wernsdorfer, W.; Folting, K.; Pink, M.; Christou, G. *J. Am. Chem. Soc.* **2004**, *126*, 2156. (b) Murugesu, M.; Habrych, M.; Wernsdorfer, W.; Abboud, K. A.; Christou, G. *J. Am. Chem. Soc.* **2004**, *126*, 4766.
(12) Tasiopoulos, A. J.; Vinslava, A.; Wernsdorfer, W.; Abboud, K. A.; Christou, G. *Angew. Chem., Int. Ed.* **2004**, *43*, 2117.
(13) (a) Artus, P.; Boskovic, C.; Yoo, Y.; Streib, W. E.; Brunel, L.-C.; Hendrickson, D. N.; Christou, G. *Inorg. Chem.* **2001**, *40*, 4199. (b) Ruiz, D.; Sun, Z.; Albela, B.; Folting, K.; Ribas, J.; Christou, G.; Hendrickson, D. N. *Angew. Chem., Int. Ed. Engl.* **1998**, *37*, 300. (c) Aubin, S. M. J.; Sun, Z.; Guzei, I. A.; Rheingold, A. L.; Christou, G.; Hendrickson, D. N. *J. Chem. Soc., Chem. Commun.* **1997**, 2239. (d) Boskovic, C.; Pink, M.; Huffman, J. C.; Hendrickson, D. N.; Christou, G. *J. Am. Chem. Soc.* **2001**, *123*, 9914. (e) Soler, M.; Artus, P.; Folting, K.; Huffman, J. C.; Hendrickson, D. N.; Christou, G. *Inorg. Chem.* **2001**, *40*, 4902.
(14) (a) Wang, S.; Huffman, J. C.; Folting, K.; Streib, W. E.; Lobkovsky, E.; Christou, G. *Angew. Chem., Int. Ed. Engl.* **1991**, *30*, 1672. (b) Tsai, L.; Wang, S.; Folting, K.; Streib, W. E.; Hendrickson, D. N.; Christou, G. *J. Am. Chem. Soc.* **1995**, *117*, 2503.
(15) (a) Bhaduri, S.; Tasiopoulos, A.; Pink, M.; Abboud, K. A.; Christou, G. *Chem. Commun.* **2002**, 2352. (b) Canada-Vilalta, C.; Pink, M.; Christou, G. *J. Chem. Soc., Dalton Trans.* **2003**, 1121.
(16) (a) Eppley, H. J.; Tsai, H. L.; de Vries, N.; Folting, K.; Christou, G.; Hendrickson, D. N. *J. Am. Chem. Soc.* **1995**, *117*, 301. (b) Chakov, N. E.; Soler, M.; Wernsdorfer, W.; Abboud, K. A.; Christou, G. *Inorg. Chem.* **2005**, *44*, 5304. (c) Aubin, S. M. J.; Sun, Z.; Pardi, L.; Krzystek, J.; Folting, K.; Brunel, L. C.; Rheingold, A. L.; Christou, G.; Hendrickson, D. N. *Inorg. Chem.* **1999**, *38*, 5329. (d) Soler, M.; Wernsdorfer, W.; Abboud, K. A.; Huffman, J. C.; Davidson, E. R.; Hendrickson, D. N.; Christou, G. *J. Am. Chem. Soc.* **2003**, *125*, 3576. (e) Soler, M.; Wernsdorfer, W.; Abboud, K. A.; Hendrickson, D. N.; Christou, G. *Polyhedron* **2003**, *22*, 1777. (f) Soler, M.; Chandra, S. K.; Ruiz, D.; Davidson, E. R.; Hendrickson, D. N.; Christou, G. *Chem. Commun.* **2000**, 2417. (g) Soler, M.; Chandra, S. K.; Ruiz, D.; Huffman, J. C.; Hendrickson, D. N.; Christou, G. *Polyhedron* **2001**, *20*, 1279.
(17) Aliaga, N.; Folting, K.; Hendrickson, D. N.; Christou, G. *Polyhedron* **2001**, *20*, 1273.
(18) Perlepes, S. P.; Huffman, J. C.; Christou, G. *J. Chem. Soc., Chem. Commun.* **1991**, *23*, 1657.
(19) Canada-Vilalta, C.; Huffman, J. C.; Christou, G. *Polyhedron* **2001**, *20*, 1785.
(20) (a) Stamatatos, Th. C.; Abboud, K. A.; Wernsdorfer, W.; Christou, G. *Angew. Chem., Int. Ed.* **2006**, *45*, 4134. (b) Stamatatos, Th. C.; Abboud, K. A.; Wernsdorfer, W.; Christou, G. *Angew. Chem., Int. Ed.* **2007**, *46*, 884.
(21) (a) Harden, N. C.; Bolcar, M. A.; Wernsdorfer, W.; Abboud, K. A.; Streib, W. E.; Christou, G. *Inorg. Chem.* **2003**, *42*, 7067. (b) Yoo, J.; Brechin, E. K.; Yamaguchi, A.; Nakano, M.; Huffman, J. C.; Maniero, A. L.; Brunel, L. C.; Awaga, K.; Ishimoto, H.; Christou, G.; Hendrickson, D. N. *Inorg. Chem.* **2000**, *39*, 3615. (c) Boskovic, C.; Wernsdorfer, W.; Folting, K.; Huffman, J. C.; Hendrickson, D. N.; Christou, G. *Inorg. Chem.* **2002**, *41*, 5107. (d) Yang, E.-C.; Harden, N.; Wernsdorfer, W.; Zakharov, L.; Brechin, E. K.; Rheingold, A. L.; Christou, G.; Hendrickson, D. N. *Polyhedron* **2003**, *22*, 1857. (e) Yang, E.-C.; Wernsdorfer, W.; Hill, S.; Edwards, R. S.; Nakano, M.; Maccagnano, S.; Zakharov, L. N.; Rheingold, A. L.; Christou, G.; Hendrickson, D. N. *Polyhedron* **2003**, *22*, 1727. (f) Yang, E.-C.; Hendrickson, D. N.; Wernsdorfer, W.; Nakano, M.; Zakharov, L. N.; Sommer, R. D.; Rheingold, A. L.; Ledezma-Gairraud, M.; Christou, G. *J. Appl. Phys.* **2002**, *91*, 7382.

arm attached at its 6-position. The resulting molecule, 2,6-diacetylpyridine dioxime ($dapdoH_2$), is shown in Scheme 1, where the analogy between the mpkoH/$dapdoH_2$ and hmpH/$pdmH_2$ pairs can be clearly seen. We anticipated that the use of $dapdoH_2$ in polynuclear transition metal cluster chemistry would give products distinctly different from those with mpkoH, and we have therefore explored its use initially in Mn chemistry. Note that $dapdoH_2$ has been employed to date in the literature only for the synthesis of mononuclear $[M(dapdoH_2)_2]^{2+}$ (M = Mn, Fe, Co, Ni, Cu, and Zn) complexes, containing neutral $dapdoH_2$ groups bound only through their three N atoms,[23] dinuclear $[Cu_2(dapdoH)_2]^{2+}$ where a mono-deprotonated $dapdoH^-$ N,N,N-chelates each Cu^{II} ion and links with its deprotonated arm to the neighboring Cu^{II},[24] and $[Fe(dapdoH)_2\{Fe_2OCl_4\}]$, where the two $dapdoH^-$ groups N,N,N-chelate to a Fe^{II} ion and bridge through their deprotonated arms to a Fe^{III}_2 unit.[25] In the present investigations, we have deliberately targeted higher nuclearity Mn products by exploring the reactions between $dapdoH_2$ and various Mn starting materials under basic conditions. This has successfully led to Mn_6 and Mn_8 cluster products containing deprotonated $dapdoH^-$ and $dapdo^{2-}$. The syntheses, structures, and magnetochemical characterization of these complexes are described in this paper.

Experimental Section

Syntheses. All manipulations were performed under aerobic conditions using chemicals and solvents as received, unless otherwise stated. $[Mn_3O(O_2CMe)_6(py)_3](ClO_4)$ (py = pyridine) was prepared as described elsewhere.[26] $dapdoH_2$ was synthesized as previously reported.[23] ***Warning****: Azide salts are potentially explosive; such compounds should be synthesized and used in small quantities, and treated with utmost care at all times.*

$[Mn_6O_2(OMe)_2(dapdo)_2(dapdoH)_4](ClO_4)_2$ (1). Method A. To a stirred brown solution of $[Mn_3O(O_2CMe)_6(py)_3](ClO_4)$ (0.18 g, 0.20 mmol) in MeOH (15 mL) was added a colorless solution of $dapdoH_2$ (0.12 g, 0.60 mmol) and NEt_3 (0.06 mL, 0.40 mmol) in MeOH (10 mL). The resulting dark brown solution was stirred for 20 min and filtered, and the filtrate was left undisturbed to concentrate slowly by evaporation. After 3 days, brown crystals of **1**·H_2O were collected by filtration, washed with cold MeOH (2 × 3 mL) and Et_2O (2 × 5 mL), and dried under vacuum; the yield was 0.13 g (~70%). Anal. Calcd for **1** (solvent-free): C, 37.92; H, 3.64; N, 14.21%. Found: C, 37.72; H, 3.59; N, 14.34%. Selected IR data (cm^{-1}): 3415 (mb), 3091 (m), 2970 (w), 2914 (w), 2800 (wb), 1637 (wb), 1595 (s), 1540 (m), 1448 (mb), 1374 (m), 1267 (m), 1094 (vs), 1056 (vs), 953 (m), 811 (m), 710 (m), 661 (m), 623 (m), 560 (s), 433 (w).

Method B. To a stirred brown solution of $[Mn_3O(O_2CMe)_6(py)_3](ClO_4)$ (0.18 g, 0.20 mmol) in MeOH (25 mL) was added solid $dapdoH_2$ (0.12 g, 0.60 mmol). The resulting dark brown solution was stirred for 45 min, during which time all the $dapdoH_2$ had dissolved. The solution was filtered and the filtrate layered with Et_2O (50 mL). After 2 days, brown crystals were collected by filtration, washed with cold MeOH (2 × 3 mL) and Et_2O (2 × 5 mL), and dried under vacuum; the yield was 0.07 g (~40%). The identity of the product was confirmed by elemental analysis (C, H, N) and IR spectroscopic comparison with material from method A.

$[Mn_6O_2(OMe)_2(dapdo)_2(dapdoH)_4][Ca(NO_3)_4]$ (2). To a stirred solution of $Mn(NO_3)_2$·H_2O (0.09 g, 0.50 mmol) and $Ca(NO_3)_2$·$4H_2O$ (0.06 g, 0.25 mmol) in MeOH (15 mL) was added a solution of $dapdoH_2$ (0.10 g, 0.50 mmol) and NEt_3 (0.07 mL, 0.50 mmol) in MeOH (10 mL). The resulting dark brown solution was stirred for 20 min and filtered, and the filtrate was layered with Et_2O (50 mL). After 5 days, brown crystals of **2**·*x*(solv) were collected by filtration, washed with cold MeOH (2 × 3 mL) and Et_2O (2 × 5 mL), and dried under vacuum; the yield was 0.10 g (~60%). Anal. Calcd for **2** (solvent-free): C, 36.10; H, 3.46; N, 16.54%. Found: C, 36.20; H, 3.80; N, 16.44%. Selected IR data (cm^{-1}): 3393 (mb), 3092 (m), 2975 (m), 2800 (wb), 1636 (m), 1596 (s), 1541 (m), 1488 (m), 1382 (vs), 1267 (m), 1200 (m), 1140 (s), 1057 (vs), 950 (m), 810 (m), 782 (w), 744 (w), 714 (m), 660 (s), 557 (s), 426 (w).

$[Mn_8O_4(OH)_4(OMe)_2(N_3)_2(dapdo)_2(dapdoH)_2(H_2O)_2]$ (3). To a stirred solution of $dapdoH_2$ (0.10 g, 0.50 mmol) and NEt_3 (0.14 mL, 1.00 mmol) in MeOH (20 mL) was added solid $MnCl_2$·$4H_2O$ (0.20 g, 1.00 mmol). The resulting brown solution was stirred for 15 min, during which time solid NaN_3 (0.04 g, 0.50 mmol) was added in small portions. The solution was stirred for a further 30 min and filtered, and the filtrate was left undisturbed to concentrate slowly by evaporation. After 2 days, dark brown crystals of **3**·*x*H_2O were collected by filtration, washed with cold MeOH (2 × 3 mL) and Et_2O (2 × 5 mL), and dried under vacuum over silica gel; the yield was 0.11 g (~55%). Dried material is hygroscopic and analyzed as **3**·$3H_2O$. Anal. Calcd for **3**·$3H_2O$: C, 28.99; H, 3.71; N, 16.01%. Found: C, 29.25; H, 3.97; N, 16.41%. Selected IR data (cm^{-1}): 3433 (sb), 2923 (m), 2077 (vs), 1635 (mb), 1599 (m), 1544 (m), 1458 (mb), 1373 (m), 1286 (w), 1194 (w), 1131 (m), 1048 (vs), 959 (m), 808 (m), 715 (m), 665 (m), 613 (sb), 566 (mb), 413 (w).

X-ray Crystallography. Data were collected on a Bruker SMART PLATFORM equipped with a CCD area detector and a graphite monochromator utilizing Mo Kα radiation. Suitable crystals were attached to glass fibers using silicone grease and transferred to a goniostat where they were cooled to 90 K for data collection. An initial search of reciprocal space revealed triclinic (**1**·H_2O), tetragonal (**2**·*x*(solv)), and monoclinic (**3**·*x*H_2O) cells; the choices of space groups $P\bar{1}$, $P4/n$, and $P2_1$, respectively, were confirmed by the subsequent solution and refinement of the structures. Cell parameters were refined using up to 999 reflections. A full sphere of data (1800 frames) was collected using the ω-scan method (0.300° frame width). Absorption corrections by integration were applied on the basis of measured indexed crystal faces. The structures were solved by direct methods in *SHELXS-86*,[27] and refined on F^2 by full-matrix least-squares techniques with *SHELXL-97*.[28] The non-H atoms were treated anisotropically, whereas the H atoms were placed in calculated, ideal positions and refined as

(22) (a) Stamatatos, Th. C.; Foguet-Albiol, D.; Stoumpos, C. C.; Raptopoulou, C. P.; Terzis, A.; Wernsdorfer, W.; Perlepes, S. P.; Christou, G. *J. Am. Chem. Soc.* **2005**, *127*, 15380. (b) Stamatatos, Th. C.; Foguet-Albiol, D.; Lee, S. C.; Stoumpos, C. C.; Raptopoulou, C. P.; Terzis, A.; Wernsdorfer, W.; Hill, S.; Perlepes, S. P.; Christou, G. *J. Am. Chem. Soc.* **2007**, *129*, 9484.

(23) Glynn, C. W.; Turnbull, M. M. *Transition Met. Chem.* **2002**, *27*, 822.

(24) (a) Nichoslon, G. A.; Lazarus, C. R.; McCormick, B. J. *Inorg. Chem.* **1980**, *19*, 192. (b) Nichoslon, G. A.; Lazarus, C. R.; McCormick, B. J. *Inorg. Chem.* **1980**, *19*, 195.

(25) Vasilevsky, I.; Stempkamp, R. E.; Lingafelter, E. C.; Rose, N. J. *J. Coord. Chem.* **1988**, *19*, 171.

(26) Vincent, J. B.; Chang, H.-R.; Folting, K.; Huffman, J. C.; Christou, G.; Hendrickson, D. N. *J. Am. Chem. Soc.* **1987**, *109*, 5703.

(27) Sheldrick, G. M. *SHELXS-86: Structure Solving Program*; University of Göttingen: Göttingen, Germany, 1986.

(28) Sheldrick, G. M. *SHELXL-97: Crystal Structure Refinement Program*; University of Göttingen: Göttingen, Germany, 1997.

Table 1. Crystallographic Data for **1**·H_2O, **2**·*x*(solv), and **3**·*x*H_2O

	1	**2**	**3**
formula[a]	$C_{56}H_{66}Cl_2Mn_6N_{18}O_{25}$	$C_{56}H_{64}CaMn_6N_{22}O_{28}$	$C_{38}H_{52}Mn_8N_{18}O_{20}$
fw,[a] g mol^{-1}	1791.79	1862.97	1520.45
crystal system	triclinic	tetragonal	monoclinic
space group	$P\bar{1}$	$P4/n$	$P2_1$
α, Å	11.3405(15)	24.3751(12)	13.3236(16)
b, Å	13.0773(18)	24.3751(12)	19.432(2)
c, Å	13.6561(19)	14.1764(10)	13.3786(16)
α, deg	66.664(2)		
β, deg	79.922(2)		105.572(2)
γ, deg	83.865(2)		
V, Å^3	1829.3(4)	8422.8(8)	3336.7(7)
Z	2	2	2
T, °C	90(2)	90(2)	90(2)
radiation,[b] Å	0.71073	0.71073	0.71073
ρ_{calc}, g cm^{-3}	1.639	1.556	1.637
μ, mm^{-1}	1.168	1.027	1.552
R1[c,d]	0.0517	0.0602	0.0967
wR2[e]	0.1305	0.1687	0.2345

[a] Including solvate molecules. [b] Graphite monochromator. [c] $I > 2\sigma(I)$. [d] $R1 = \sum(||F_o| - |F_c||)/\sum|F_o|$. [e] $wR2 = [\sum[w(F_o^2 - F_c^2)^2]/\sum[w(F_o^2)^2]]^{1/2}$, $w = 1/[\sigma^2(F_o^2) + [(0.0680p)^2 + 3.6073p]$, where $p = [\max(F_o^2, 0) + 2F_c^2]/3$.

riding on their respective C atoms. Hydrogen atoms bonded to oxygen were generated in the Fourier difference map and constrained to ride on the positions of the parent atoms. Unit cell parameters and structure solution and refinement data are listed in Table 1.

For **1**·H_2O, the asymmetric unit contains half the Mn_6 cation, one ClO_4^- anion, and one H_2O molecule of crystallization disordered over two positions. A total of 490 parameters were included in the structure refinement using 8899 reflections with $I > 2\sigma(I)$ to yield R1 and wR2 of 5.17% and 13.05%, respectively. For **2**·*x*(solv), the asymmetric unit contains half the Mn_6 cation, two $^1/_4Ca(NO_3)_4^{2-}$ anions, and several disordered MeOH, Et_2O, and H_2O molecules of crystallization. A total of 580 parameters were included in the structure refinement using 7453 reflections with $I > 2\sigma(I)$ to yield R1 and wR2 of 6.02% and 16.87%, respectively. For **3**·*x*H_2O, the asymmetric unit contains the complete Mn_8 cluster, and several disordered solvent molecules of crystallization. Two charge compensating azide ligands are exohedrally bound to the cluster. One of the azides is disordered over two positions with bound solvent. The occupancies of the disordered azide and coordinated solvent were refined as a free variable. The crystal is racemically twinned and was refined as such with a batch scale factor of 0.6332. A total of 791 parameters were included in the structure refinement using 15252 reflections with $I > 2\sigma(I)$ to yield R1 and wR2 of 9.67% and 23.45%, respectively. The refinement of complex **3** results in a somewhat large R1 value of 9.67% as a consequence of disorder in the structure, the large amount of solvent accessible space, and the presence of racemic twinning in the crystal.

Physical Measurements. Infrared spectra were recorded in the solid state (KBr pellets) on a Nicolet Nexus 670 FTIR spectrometer in the 400−4000 cm^{-1} range. Elemental analyses (C, H, and N) were performed by the in-house facilities of the University of Florida Chemistry Department. Variable-temperature dc and ac magnetic susceptibility data were collected at the University of Florida using a Quantum Design MPMS-XL SQUID susceptometer equipped with a 7 T magnet and operating in the 1.8−300 K range. Samples were embedded in solid eicosane to prevent torquing. Magnetization versus field and temperature data were fit using the program MAGNET.[29] Pascal's constants were used to estimate the diamagnetic corrections, which were subtracted from the experimental susceptibilities to give the molar paramagnetic susceptibilities (χ_M).

Results and Discussion

Syntheses. Many synthetic procedures to make polynuclear manganese clusters rely on the reaction of triangular $[Mn_3O(O_2CR)_6L_3]^+$ species with a potentially chelating ligand. In particular, hmpH, related 2-(hydroxyethyl)-pyridine (hepH), and $pdmH_2$ have given products such as $[Mn_{10}O_4(OH)_2(O_2CMe)_8(hmp)_8]^{4+}$,[21a] $[Mn_{18}O_{14}(O_2CMe)_{18}(hep)_4(hepH)_2(H_2O)_2]^{2+}$,[30] and $[Mn_4(O_2CMe)_2(pdmH)_6]^{2+}$.[31] We thus explored this starting material for reactions with $dapdoH_2$. In addition, this would provide a useful comparison between $dapdoH_2$ and mpkoH, since the latter reacts with $[Mn_3O(O_2CR)_6(py)_3]^+$ in a 3:1 molar ratio to give $[Mn_3O(O_2CR)_3(mpko)_3]^+$.[22] Thus, we carried out the reaction between 3 equiv of $dapdoH_2$ and $[Mn_3O(O_2CMe)_6(py)_3](ClO_4)$ in MeOH, and from the resulting dark brown solution were obtained well-formed brown crystals of $[Mn_6O_2(OMe)_2(dapdo)_2(dapdoH)_4](ClO_4)_2$ (**1**; $2Mn^{II}$, $4Mn^{III}$) in good yields (∼40%). The formation of **1** is summarized in eq 1; the electrons required to give the Mn^{II} ions in **1** are assumed to result from oxidation of MeOH.

$$2[Mn_3O(O_2CMe)_6(py)_3]^+ + 6dapdoH_2 + 2MeOH + 2e^- \rightarrow 12MeCO_2^- + 10H^+ + 6py + [Mn_6O_2(OMe)_2(dapdo)_2(dapdoH)_4]^{2+} \quad (1)$$

We also investigated the identity of the product as a function of the carboxylate groups on the Mn_3 starting material, but we obtained the analogous product to **1** in every case. Complex **1** was also the only isolable product from a variety of other reactions in MeOH with differing reagent ratios, amounts of base, and other conditions; however, the addition of 1−3 equiv of NEt_3 did at least increase the yield of **1** to ∼70%. On the other hand, an increase in the $dapdoH_2$:Mn_3 ratio to 5:1 (or greater) in MeOH did not give **1** but instead gave yellow solutions from which were subsequently isolated yellow crystals of the perchlorate salt of known mononuclear $[Mn^{II}(dapdoH_2)_2]^{2+}$.[23] At the other extreme, large Mn_3:$dapdoH_2$ ratios in MeOH led to the known, $dapdoH_2$-free cluster $[Mn_{84}O_{72}(OMe)_{24}(O_2CMe)_{78}(MeOH)_{12}(H_2O)_{42}]$.[12]

The reaction to complex **1** was also investigated as a potential route to heterometallic Mn/Ca clusters that might be of potential relevance to the bioinorganic importance of Mn, as mentioned in the Introduction. We recently reported the first intimately associated Mn/Ca and Mn/Sr clusters

(29) Davidson, E. R. *MAGNET*; Indiana University: Bloomington, IN, 1999.
(30) Brechin, E. K.; Sanudo, E. C.; Wernsdorfer, W.; Boskovic, C.; Yoo, J.; Hendrickson, D. N.; Yamaguchi, A.; Ishimoto, H.; Concolino, T. E.; Rheingold, A. L.; Christou, G. *Inorg. Chem.* **2005**, *44*, 502.
(31) Brechin, E. K.; Yoo, J.; Huffman, J. C.; Hendrickson, D. N.; Christou, G. *Chem. Commun*. **1999**, 783.

containing Mn^{III},[32] and wondered whether the synthesis of $Mn^{II}_2Mn^{III}_4$ complex **1** could be modified to perhaps provide the corresponding $Ca^{II}_2Mn^{III}_4$ cluster. Thus, several reactions have been investigated in MeOH with a Mn:Ca:dapdoH$_2$ ratio of 2:1:2, among others, and the only isolable product was $[Mn_6O_2(OMe)_2(dapdo)_2(dapdoH)_4][Ca(NO_3)_4]$ (**2**), whose cation is identical to that in **1**.

Since complex **1** contains bridging methoxide groups, a similar reaction was carried out in the presence of sodium azide. Perlepes and co-workers have demonstrated that the replacement of bridging hydroxide groups (which almost always mediate antiferromagnetic exchange) with end-on azide groups (which mediate ferromagnetic exchange) in cobalt, nickel, and iron clusters leads to isostructural products with much higher ground-state spin values.[33] Thus, we explored a variety of reactions differing in the azide amount, the Mn:dapdoH$_2$:NEt$_3$ ratio, and/or the solvent, and it was found that the reaction of $MnCl_2 \cdot 4H_2O$, dapdoH$_2$, NEt$_3$, and NaN_3 in a 2:1:2:1 ratio gave the new octanuclear complex $[Mn_8O_4(OH)_4(OMe)_2(N_3)_2(dapdo)_2(dapdoH)_2(H_2O)_2]$ (**3**) in good yields (~55%). The formation of **3** is summarized in eq 2.

$$8Mn^{2+} + 4dapdoH_2 + 20NEt_3 + 2N_3^- + 2MeOH + 10H_2O \rightarrow [Mn_8O_4(OH)_4(OMe)_2(N_3)_2(dapdo)_2(dapdoH)_2(H_2O)_2] + 20NHEt_3^+ + 6e^- \quad (2)$$

In fact, complex **3** has only terminal azide groups, but it nevertheless has a new and interesting core structure. Complex **3** was also obtained in lower yield from the reaction of preformed complex **1** with 3−5 equiv of sodium azide in MeOH.

Description of Structures. A partially labeled representation and a stereoview of the cation of complex **1** are shown in Figure 1. Selected interatomic distances and angles are listed in Table 2. Complex **1** crystallizes in triclinic space group $P\bar{1}$ and possesses crystallographic C_i symmetry. Complex **2** contains the same cation as **1**, and a $[Ca(NO_3)_4]^{2-}$ counterion, and will not be further discussed. The core of **1** consists of six Mn ions arranged as two edge-sharing tetrahedra (Figure 2, top), each with a central μ_4-O^{2-} ion (O7, O7′). The Mn−μ_4-O^{2-}−Mn angles range from 95.7(8)° to 119.0(1)°, deviating significantly from the 109.5° ideal values of a tetrahedron. The Mn atoms are additionally bridged by eight NO^- oximate groups of two dapdo^{2-} and four dapdoH$^-$ chelates. The dapdo^{2-} groups are tridentate-chelating to a Mn^{II} atom, with each of their alkoxide arms also bridging to adjacent Mn^{III} atoms; these groups are thus $\eta^1{:}\eta^1{:}\eta^1{:}\eta^1{:}\eta^1{:}\mu_3$ (Scheme 2). The dapdoH$^-$ groups are tridentate-chelating to a Mn^{III} atom, but only the deprotonated N−O$^-$ arm bridges to an adjacent Mn^{II} or Mn^{III} atom; these groups are thus $\eta^1{:}\eta^1{:}\eta^1{:}\eta^1{:}\mu$ (Scheme 2). In addition, there are two MeO$^-$ groups (O8M and O8′M) bridging Mn1 and Mn3. The complex thus contains a $[Mn_6(\mu_4\text{-}O)_2(\mu\text{-}OMe)_2(\mu\text{-}ON)_8]^{2+}$ core (Figure 2, bottom). Mn2, Mn2′, Mn3, and Mn3′ are six-coordinate with distorted octahedral geometry, whereas Mn1 and Mn1′ are seven-coordinate with distorted pentagonal bipyramidal geometry. Charge considerations indicate a mixed-valence $Mn^{II}_2Mn^{III}_4$ description, and the Mn^{III} centers are assigned as the external Mn2 and Mn3 on the basis of the metric parameters and bond valence sum

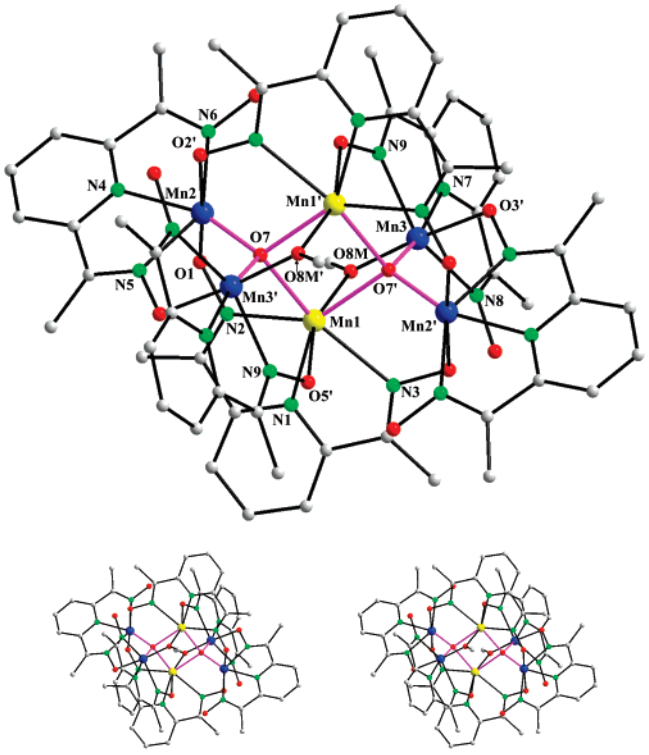

Figure 1. Labeled PovRay representation (top) and stereopair (bottom) of complex **1**, with H atoms omitted for clarity.

Table 2. Selected Interatomic Distances (Å) and Angles (deg) for **1**·H$_2$O[a]

Mn(1)···Mn(2)	3.629(3)	Mn(1)···Mn(3)	3.581(3)
Mn(1)···Mn(3)	3.214(2)	Mn(2)···Mn(3)	5.213(3)
Mn(1)···Mn(2)	3.453(2)	Mn(2)···Mn(3)	3.122(4)
Mn(1)−O(5)	2.234(2)	Mn(1)···Mn(1)	3.365(5)
Mn(1)−O(7)	2.331(2)	Mn(2)−N(4)	2.143(3)
Mn(1)−O(7)	2.206(2)	Mn(2)−N(5)	2.216(2)
Mn(1)−O(8M)	2.202(2)	Mn(2)−N(6)	2.273(3)
Mn(1)−N(1)	2.315(3)	Mn(3)−O(3)	1.937(2)
Mn(1)−N(2)	2.261(3)	Mn(3)−O(7)	1.943(2)
Mn(1)−N(3)	2.380(3)	Mn(3)−O(8M)	1.871(2)
Mn(2)−O(1)	1.890(2)	Mn(3)−N(7)	2.140(2)
Mn(2)−O(2)	1.949(2)	Mn(3)−N(8)	2.364(3)
Mn(2)−O(7)	1.872(2)	Mn(3)−N(9)	2.180(3)

Mn(1)−O(7)−Mn(2)	119.0(1)	Mn(1)−O(7)−Mn(2)	115.5(1)
Mn(1)−O(7)−Mn(3)	113.5(1)	Mn(1)−O(8M)−Mn(3)	103.9(1)
Mn(1)−O(7)−Mn(1)	95.7(8)	Mn(2)−O(7)−Mn(3)	109.8(1)
Mn(1)−O(7)−Mn(3)	101.3(1)		

[a] Primed and unprimed atoms are related by symmetry.

(32) (a) Mishra, A; Yano, J.; Pushkar, Y.; Yachandra, V. K.; Abboud, K. A.; Christou, G. *Chem. Commun.* **2007**, 1538. (b) Mishra, A; Wernsdorfer, W.; Abboud, K. A.; Christou, G. *Chem. Commun.* **2005**, 54.

(33) (a) Boudalis, A. K.; Donnadieu, B.; Nastopoulos, V.; Clemente-Juan, J. M.; Alain, M.; Sanakis, Y.; Tuchagues, J. P.; Perlepes, S. P. *Angew. Chem., Int. Ed.* **2004**, *43*, 2266. (b) Papaefstathiou, G. S.; Perlepes, S. P.; Escuer, A.; Vicente, R.; Font-Bardia, M.; Solans, X. *Angew. Chem., Int. Ed.* **2001**, *40*, 884. (c) Papaefstathiou, G. S.; Escuer, A.; Vicente, R.; Font-Bardia, M.; Solans, X.; Perlepes, S. P. *Chem. Commun.* **2001**, 2414.

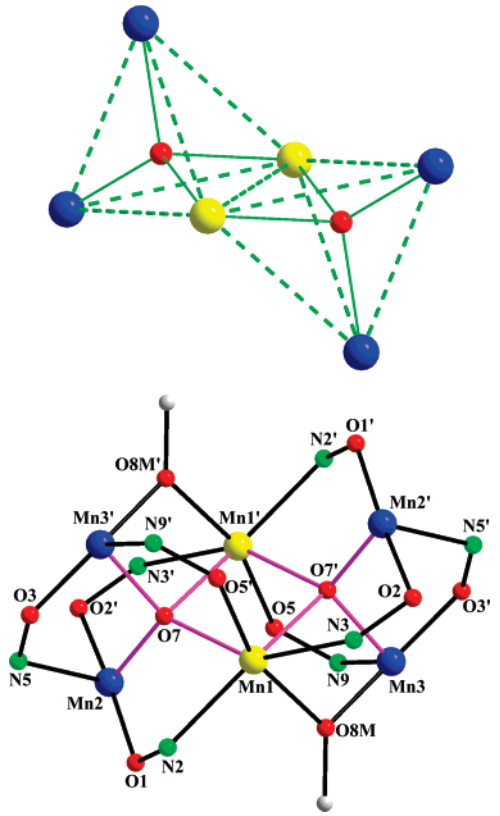

Figure 2. (top) Mn_6 topology, emphasizing the bitetrahedral description (green dashed lines), and the $[Mn_6(\mu_4\text{-}O)_2]^{12+}$ subcore (green thick lines), respectively. (bottom) PovRay representation of the complete $[Mn_6(\mu_4\text{-}O)_2(\mu\text{-}OMe)_2(\mu\text{-}NO)_8]^{2+}$ core of **1**. Color scheme: Mn^{II}, yellow; Mn^{III}, blue; O, red; N, green; C, gray.

Table 3. Bond Valence Sum (BVS)[a,b] Calculations for Mn and Selected Oxygen Atoms in **1**

atom	Mn^{II}	Mn^{III}	Mn^{IV}
Mn1	*2.026*	1.899	1.920
Mn2	3.212	*2.998*	3.049
Mn3	3.109	*2.903*	2.951

	BVS	assignment
O7	1.70	O^{2-}
O8M	1.88	MeO^-

[a] The italicized value is the one closest to the charge for which it was calculated. The oxidation state of a particular atom can be taken as the nearest whole number to the italicized value. [b] A BVS in the ~1.8−2.0, ~1.0−1.2, and ~0.2−0.4 ranges for an O atom is indicative of non-, single-, and double-protonation, respectively, but can be altered somewhat by hydrogen bonding.

(BVS) values[34] listed in Tables 2 and 3, respectively. BVS calculations also confirm that the central O1 and O1′ atoms are O^{2-} ions (Table 3). The Mn^{II} pair is consequently bridged by two μ_4-O^{2-} whereas each $Mn^{II}Mn^{III}$ and $Mn^{III}Mn^{III}$ pair is bridged by only one μ_4-O^{2-}. The four Mn^{III} atoms also show the Jahn−Teller (JT) distortion expected for a high-spin d^4 ion in near-octahedral geometry, taking the form of an axial elongation with the oximate nitrogen atoms N(5, 6 and 8, 9) of the $dapdoH^-$ groups occupying the axial positions of the Mn2 and Mn3 distorted octahedra, respectively. Thus, as is almost always the case, the JT elongation axes avoid the Mn^{III}−O^{2-} bonds, the shortest and strongest in the cation.[35]

Scheme 2. Coordination Modes of $dapdoH^-$ and $dapdo^{2-}$ in Complexes **1**−**3**

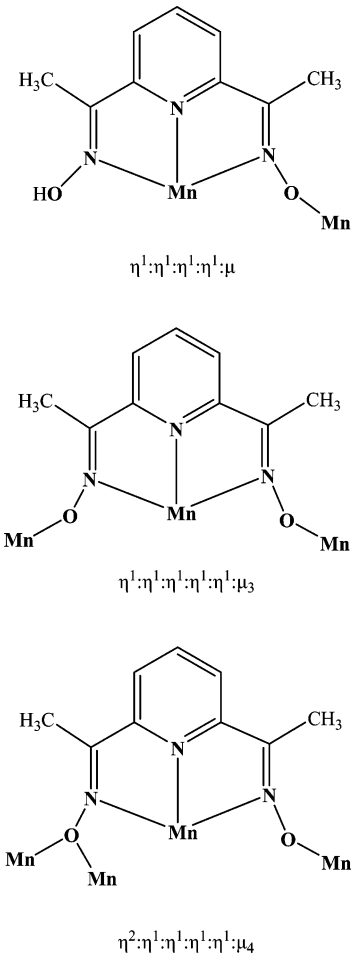

In addition to the "edge-sharing tetrahedra" description of the Mn_6O_2 core (Figure 2), two alternative ways of describing it can be presented that emphasize its structural relationship to smaller nuclearity Mn/O units: (i) The Mn_6O_2 unit can be considered as two $[Mn_3O]^{6+}$ units, joined together by each of the μ_3-O^{2-} atoms becoming μ_4 by ligating to the Mn^{II} center of the adjacent Mn_3O unit. The two $[Mn^{II}Mn^{III}_2O]^{6+}$ units comprising the $\{Mn_6O_2\}^{12+}$ core of **1** are Mn(1, 2, 3′)O(7) and Mn(1′, 2′, 3)O(7′) or, alternatively, Mn(1′, 2, 3′)O(7) and Mn(1, 2′, 3)O(7′). (ii) The $\{Mn_6O_2\}^{12+}$ core can be considered to contain the $[Mn^{II}_2Mn^{III}_2O_2]$ core of $[Mn_4O_2(O_2CMe)_6(bpy)_2]$.[36] The latter possesses a planar-butterfly (Mn_4 rhombus) topology with two Mn^{III} atoms at the central ("body") and two Mn^{II} atoms on its end ("wingtip") positions, with the two μ_3-O^{2-} bridges one above and one below the plane. This unit is to be found within **1** (Mn(1, 1′, 2, 2′)O(7, 7′)) or Mn(1, 1′, 3, 3′)O(7, 7′)), and

(34) (a) Brown, I. D.; Altermatt, D. *Acta Crystallogr.* **1985**, *B41*, 244. (b) Liu, W.; Thorp, H. H. *Inorg. Chem.* **1993**, *32*, 4102.

(35) Chakov, N. E.; Lee, S.-C.; Harter, A. G.; Kuhns, P. L.; Reyes, A. P.; Hill, S. O.; Dalal, N. S.; Wernsdorfer, W.; Abboud, K. A.; Christou, G. *J. Am. Chem. Soc.* **2006**, *128*, 6975.

(36) Vincent, J. B.; Christmas, C.; Chang, H.-R.; Li, Q.; Boyd, P. D. W.; Huffman, J. C.; Hendrickson, D. N.; Christou, G. *J. Am. Chem. Soc.* **1989**, *111*, 2086.

completion of the Mn_6O_2 core then requires merely the conversion of the two μ_3-O^{2-} to μ_4-O^{2-} by ligation to an additional Mn^{III} center. Note that on the central Mn_4 rhombus of **1** the Mn^{II} and Mn^{III} atoms have switched their locations; i.e., the former occupy the "body" and the latter the "wingtip" positions.

The structure of **1** also contains four strong intramolecular OH···H hydrogen-bonds between the protonated N−OH group of each dapdoH$^-$ chelate and the deprotonated N−O− group of a neighboring dapdoH$^-$ chelate: O(4)···O(5) = 2.565(4) Å, O(6)···O(2) = 2.610(4) Å. There are no significant intermolecular hydrogen-bonds, only weak ones involving C−H bonds.

Compounds **1** and **2** are only the second and third Mn_6 complexes comprising $2Mn^{II}$ and $4Mn^{III}$ atoms, and the first ones with the $[Mn^{II}_2Mn^{III}_4(\mu_4\text{-}O)_2]^{12+}$ edge-sharing bitetrahedral core. The one previous Mn_6 at this oxidation level is $[Mn_6O_2(O_2CPh)_{12}(py)_2]$, which has a core consisting of two $[Mn_3(\mu_3\text{-}O)]^{6+}$ triangular units linked together by bridging $PhCO_2^-$ groups.[37] It should be added, however, that Mn_6 complexes with an edge-sharing bitetrahedral $[Mn_6(\mu_4\text{-}O)_2]^{n+}$ core are much more common at the $Mn^{II}_4Mn^{III}_2$ oxidation level; these have a general formula of $[Mn_6O_2(O_2CR)_{10}L_4]$, where L is a neutral group such as MeCN, py, etc.[38] In these complexes, the two Mn^{III} atoms occupy the central positions, and the four Mn^{II} atoms occupy the end sites, the opposite situation to that seen in **1** (and **2**). The magnetic properties of the $[Mn^{II}_4Mn^{III}_2(\mu_4\text{-}O)_2]^{10+}$ complexes are dominated by antiferromagnetic exchange interactions, leading to a diamagnetic $S = 0$ ground state.

A labeled representation of complex **3** is shown in Figure 3. Selected interatomic distances and angles are given in Table 4. Complex **3** crystallizes in the monoclinic space group $P2_1$ with the Mn_8 molecule in a general position. The structure consists of an $[Mn_8(\mu_4\text{-}O)_2(\mu_3\text{-}O)_2]^{14+}$ core (Figure 4, top) that may be conveniently described as two $[Mn_4O_2]$ planar-butterfly units (Mn(1, 3, 7, 8) and Mn(2, 4, 5, 6)) linked by one μ_3-O^{2-} ion in each unit converting to a μ_4 mode and thus providing the two interbutterfly bonds, Mn1−O10 and Mn2−O9. The coordination geometry at O9 and O10 is thus distorted tetrahedral, while that at O11 and O12 is essentially trigonal planar (slightly trigonal pyramidal). Peripheral ligation about the core is provided by four μ-OH^- (O13, O14, O15, and O16), two μ-OMe^- (O17M and O18M), two η^1:η^1:η^1:η^1:μ-dapdoH$^-$, and two η^2:η^1:η^1:η^1:η^1:μ_4-dapdo^{2-} groups (Scheme 2). The dapdo^{2-} groups are tridentate-chelating to a Mn^{III} atom, with their N−O$^-$ arms bound to an adjacent Mn atom and one of them bridging two Mn atoms. The dapdoH$^-$ groups are again tridentate-chelating to a Mn^{III} atom, but only the deprotonated N−O$^-$ arm is also bound to an adjacent Mn atom. Terminal azide and water groups complete ligation on Mn8 and Mn5, respectively. A second pair of terminal azide and water

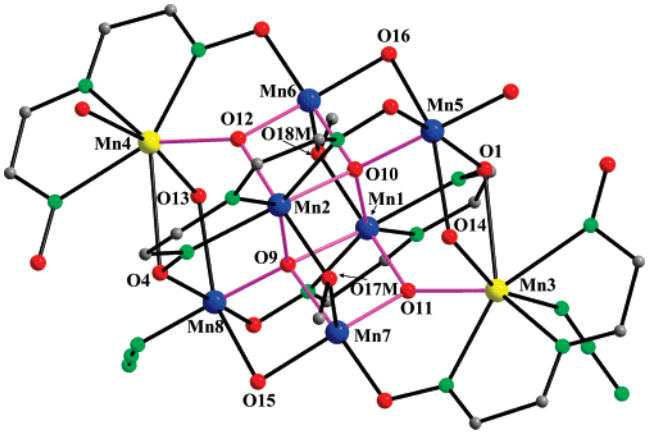

Figure 3. Labeled PovRay representation of complex **3**, with some of the dioxime C atoms and all H atoms omitted for clarity; only one of the azide/water disorder situations between Mn3 and Mn4 is shown.

Table 4. Selected Interatomic Distances (Å) and Angles (deg) for **3**·xH$_2$O

Mn(1)−O(9)	2.018(9)	Mn(4)−N(10)	2.304(1)
Mn(1)−O(10)	2.326(9)	Mn(4)−N(11)	2.308(1)
Mn(1)−O(11)	1.816(1)	Mn(4)−N(12)	2.469(2)
Mn(1)−O(18M)	1.956(1)	Mn(4)−N(16A)	2.427(2)
Mn(1)−N(1)	2.265(7)	Mn(5)−O(1)	1.950(1)
Mn(1)−N(2)	2.177(1)	Mn(5)−O(3)	1.899(1)
Mn(1)−N(3)	2.449(1)	Mn(5)−O(10)	1.907(9)
Mn(2)−O(9)	2.357(8)	Mn(5)−O(14)	2.450(1)
Mn(2)−O(10)	2.007(1)	Mn(5)−O(16)	2.263(1)
Mn(2)−O(12)	1.862(1)	Mn(5)−O(19W)	1.899(1)
Mn(2)−O(17M)	1.945(9)	Mn(6)−O(7)	1.902(1)
Mn(2)−N(4)	2.289(7)	Mn(6)−O(10)	1.872(1)
Mn(2)−N(5)	2.421(1)	Mn(6)−O(12)	1.829(9)
Mn(2)−N(6)	2.131(1)	Mn(6)−O(16)	1.913(1)
Mn(3)−O(1)	2.684(1)	Mn(6)−O(18M)	2.195(1)
Mn(3)−O(11)	2.149(1)	Mn(7)−O(6)	1.897(9)
Mn(3)−O(14)	2.217(1)	Mn(7)−O(9)	1.898(1)
Mn(3)−O(37A)	2.477(2)	Mn(7)−O(11)	1.890(1)
Mn(3)−N(7)	2.269(1)	Mn(7)−O(15)	1.970(1)
Mn(3)−N(8)	2.440(2)	Mn(7)−O(17M)	2.099(9)
Mn(3)−N(9)	2.355(1)	Mn(8)−O(2)	1.866(9)
Mn(3)−N(19A)	2.125(2)	Mn(8)−O(4)	1.895(1)
Mn(4)−O(4)	2.800(1)	Mn(8)−O(9)	1.869(9)
Mn(4)−O(12)	2.147(1)	Mn(8)−O(13)	2.436(1)
Mn(4)−O(13)	2.189(1)	Mn(8)−O(15)	2.293(1)
Mn(4)−O(38A)	2.259(2)	Mn(8)−N(13A)	1.946(1)

Mn(1)−O(9)−Mn(2)	105.7(4)	Mn(2)−O(12)−Mn(4)	129.0(5)
Mn(1)−O(9)−Mn(7)	92.8(4)	Mn(2)−O(12)−Mn(6)	100.1(5)
Mn(1)−O(9)−Mn(8)	131.7(5)	Mn(2)−O(17M)−Mn(7)	103.2(4)
Mn(1)−O(10)−Mn(2)	107.2(4)	Mn(3)−O(1)−Mn(5)	102.6(5)
Mn(1)−O(10)−Mn(5)	116.2(5)	Mn(3)−O(11)−Mn(7)	116.8(5)
Mn(1)−O(10)−Mn(6)	97.5(4)	Mn(3)−O(14)−Mn(5)	102.6(5)
Mn(1)−O(11)−Mn(3)	131.7(6)	Mn(4)−O(4)−Mn(8)	100.0(5)
Mn(1)−O(11)−Mn(7)	99.9(5)	Mn(4)−O(12)−Mn(6)	119.7(5)
Mn(1)−O(18M)−Mn(6)	99.4(4)	Mn(4)−O(13)−Mn(8)	103.8(4)
Mn(2)−O(9)−Mn(7)	95.8(4)	Mn(5)−O(10)−Mn(6)	104.9(5)
Mn(2)−O(9)−Mn(8)	116.3(4)	Mn(5)−O(16)−Mn(6)	91.3(5)
Mn(2)−O(10)−Mn(5)	129.4(5)	Mn(7)−O(9)−Mn(8)	105.0(5)
Mn(2)−O(10)−Mn(6)	93.6(4)	Mn(7)−O(15)−Mn(8)	88.7(5)

(37) Low, D. M.; Brechin, E. K.; Helliwell, M.; Mallah, T.; Riviere, E.; McInnes, E. J. L. *Chem. Commun.* **2003**, 2330.

(38) (a) Schake, A. R.; Vincent, J. B.; Li, Q.; Boyd, P. D. W.; Folting, K.; Huffman, J. C.; Hendrickson, D. N.; Christou, G. *Inorg. Chem.* **1989**, *28*, 1915. (b) Stamatatos, Th. C.; Foguet-Albiol, D.; Perlepes, S. P.; Raptopoulou, C. P.; Terzis, A; Patrickios, C. S.; Christou, G.; Tasiopoulos, A. J. *Polyhedron* **2006**, *25*, 1737. (c) Halcrow, M. A.; Streib, W. E.; Folting, K.; Christou, G. *Acta Crystallogr., Sect. C* **1995**, *51*, 1263. (d) Murie, M.; Parsons, S.; Winpenny, R. E. P. *J. Chem. Soc., Dalton Trans.* **1998**, 1423. (e) Baikie, A. R. E.; Howes, A. J.; Hursthouse, M. B.; Quick, A. B.; Thornton, P. *J. Chem. Soc., Chem. Commun.* **1986**, 1587. (f) Batsanov, A. S.; Struchkov, Y. T.; Timco, G. A.; Gerbeleu, N. V.; Manole, O. S.; Grebenko, S. V. *Russ. J. Coord. Chem.* **1994**, *20*, 604. (g) Blackman, A. G.; Huffman, J. C.; Lobkovsky, E. B.; Christou, G. *Polyhedron* **1992**, *11*, 251. (h) Köhler, K.; Roesky, H. W.; Noltemeyer, M.; Schmidt, H.-G.; Freire-Erdbrügger, C.; Sheldrick, G. M. *Chem. Ber.* **1993**, *126*, 921. (i) Gavrilenko, K. S.; Punin, S. V.; Cador, O.; Golhen, S.; Quahab, L.; Pavlishchuk, V. V. *Inorg. Chem.* **2005**, *44*, 5903.

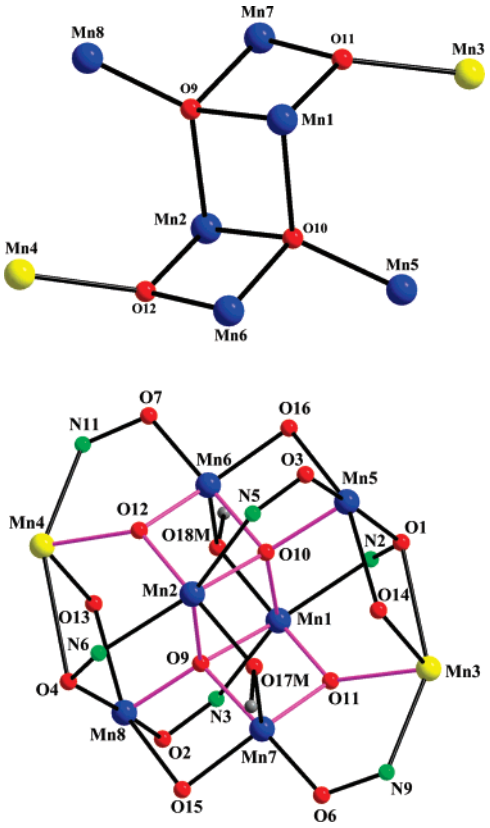

Figure 4. Labeled PovRay representations of (top) the $[Mn_8O_4]^{14+}$ core of **3**, emphasizing the linked-butterfly structure, and (bottom) the complete $[Mn_8(\mu_4\text{-}O)_2(\mu_3\text{-}O)_2(\mu\text{-}OH)_4(\mu\text{-}OMe)_2(\mu\text{-}ON)_6]^{2+}$ core. Color scheme: Mn^{II}, yellow; Mn^{III}, blue; O, red; N, green; C, gray.

Table 5. Bond Valence Sums for Mn[a] and Selected Oxygen[b] Atoms in Complex **3**

atom	Mn^{II}	Mn^{III}	Mn^{IV}
Mn1	3.127	*2.910*	2.974
Mn2	3.064	*2.854*	2.913
Mn3	*1.985*	1.883	1.868
Mn4	*1.714*	1.620	1.615
Mn5	3.098	*2.833*	2.974
Mn6	3.264	*2.985*	3.134
Mn7	3.091	*2.828*	2.969
Mn8	3.392	*3.144*	3.234

	BVS	assignment
O9	1.88	O^{2-}
O10	1.88	O^{2-}
O11	1.72	O^{2-}
O12	1.75	O^{2-}
O13	0.45	OH^-
O14	0.43	OH^-
O15	0.71	OH^-
O16	0.81	OH^-
O17M	1.70	OMe^-
O18M	1.52	OMe^-

[a] See footnote *a* of Table 3. [b] See footnote *b* of Table 3.

groups completes ligation at Mn3 and Mn4, but the ligands are disordered 50:50% between the two metals.

Charge considerations and an inspection of the metric parameters indicated a $2Mn^{II}$, $6Mn^{III}$ description for **3**. This was confirmed quantitatively by bond valence sum (BVS) calculations (Table 5),[34] which identified Mn3 and Mn4 as the Mn^{II} ions, and the others as Mn^{III}. The latter was also consistent with the Jahn−Teller (JT) axial elongations at Mn5 and Mn8, as expected for high-spin d^4 ions in near-octahedral geometry. Atoms Mn6 and Mn7 are five-coordinate with intermediate geometry ($\tau = 0.40$ and 0.44, where τ is 0 and 1 for ideal square pyramidal and trigonal bipyramidal geometries,[39] respectively). The Mn^{II} atoms and Mn^{III} atoms Mn1 and Mn2 are seven-coordinate with distorted pentagonal bipyramidal geometries. The protonation level of O^{2-}, OH^-, and OMe^- groups was confirmed by BVS calculations (Table 5). The slightly low BVS values of the four OH^- (0.43−0.81) and two OMe^- (1.52 and 1.70) groups are attributed to their participation in intra- and intermolecular O···H−O hydrogen-bonds with terminal and lattice water molecules, as well as with the uncoordinated N−OH groups of two dapdoH^- ligands.

Complex **3** joins only a small family of Mn clusters of nuclearity eight, which currently comprise the metal oxidation states Mn^{II}_8,[40] $Mn^{II}_6Mn^{III}_2$,[21c,41] $Mn^{II}_4Mn^{III}_4$,[42] $Mn^{II}_2Mn^{III}_6$,[43] Mn^{III}_8,[44] and $Mn^{III}_2Mn^{IV}_6$,[45] and thus becomes the third member of the $Mn^{II}_2Mn^{III}_6$ subfamily. The $[Mn_8O_4]$ core of **3** is similar to that in the $[Mn_8O_4(O_2CPh)_{12}(Et_2mal)_2(H_2O)_2]^{2-}$ carboxylato cluster.[43a] Complex **3** is also the first Mn_x complex to contain simultaneously bridging oxide, hydroxide, and methoxide ions.

Magnetochemistry. Magnetic Susceptibility Studies on Complex 1. Variable-temperature magnetic susceptibility measurements were performed on powdered polycrystalline samples of **1** (and **2**), restrained in eicosane to prevent torquing, in a 1 kG (0.1 T) field and in the 5.0−300 K range. The obtained data are shown as $\chi_M T$ versus T plot in Figure 5. The magnetic data for **1** and **2** are identical, and therefore only those for the former will be discussed.

$\chi_M T$ for **1** steadily decreases from 16.79 cm^3 K mol^{-1} at 300 K to a value of 9.51 cm^3 K mol^{-1} at 40 K and then increases to 12.26 cm^3 K mol^{-1} at 5.0 K. The 300 K value is much less than the spin-only ($g = 2$) value of 20.75 cm^3 K mol^{-1} for two Mn^{II} and four Mn^{III} noninteracting ions,

(39) Addison, A. W.; Rao, T. N.; Reedijk, J.; Rijn J.; Verschoor, G. C. *J. Chem. Soc., Dalton Trans.* **1984**, 1349.
(40) For example, see: (a) Saalfrank, R. W.; Löw, N.; Demleitner, B.; Stalke, D.; Teichert, M. *Chem. Eur. J.* **1998**, *4*, 1305. (b) Saalfrank, R. W.; Löw, N.; Trummer, S.; Sheldrick, G. M.; Teichert, M.; Stalke, D. *Eur. J. Inorg. Chem.* **1998**, 559.
(41) Boskovic, C.; Huffman, J. C.; Christou, G. *Chem. Commun.* **2002**, 2502.
(42) (a) Milios, C. J.; Stamatatos, Th. C.; Kyritsis, P.; Terzis, A.; Raptopoulou, C. P.; Vicente, R.; Escuer, A.; Perlepes, S. P. *Eur. J. Inorg. Chem.* **2004**, 2885. (b) Milios, C. J.; Fabbiani, F. P. A.; Parsons, S.; Murugesu, M.; Christou, G.; Brechin, E. K. *Dalton Trans.* **2006**, 351. (c) Murugesu, M.; Wernsdorfer, W.; Abboud, K. A.; Christou, G. *Angew. Chem., Int. Ed.* **2004**, *44*, 892.
(43) (a) Wemple, M. W.; Tsai, H. L.; Wang, S.; Claude, J. P.; Streib, W. E.; Huffman, J. C.; Hendrickson, D. N.; Christou, G. *Inorg. Chem.* **1996**, *35*, 6437. (b) Milios, C. J.; Inglis, R.; Vinslava, A.; Prescimone, A.; Parsons, S.; Perlepes, S. P.; Christou, G.; Brechin, E. K. *Inorg. Chem.* **2007**, *66*, 6215.
(44) For some representative references, see: (a) Libby, E.; Folting, K.; Huffman, C. J.; Huffman, J. C.; Christou, G. *Inorg. Chem.* **1993**, *32*, 2549. (b) Brechin, E. K.; Soler, M.; Christou, G.; Helliwell, M.; Teat, S. J.; Wernsdorfer, W. *Chem. Commun.* **2003**, 1276. (c) Grillo, V. A.; Knapp, M. J.; Bollinger, J. C.; Hendrickson, D. N.; Christou, G. *Angew. Chem., Int. Ed.* **1996**, *35*, 1818. (d) Tanase, S.; Aromi, G.; Bouwman, E.; Kooijman, H.; Spek, A. L.; Reedijk, J. *Chem. Commun.* **2005**, 3147.
(45) Tasiopoulos, A. J.; Abboud, K. A.; Christou, G. *Chem. Commun.* **2003**, 580.

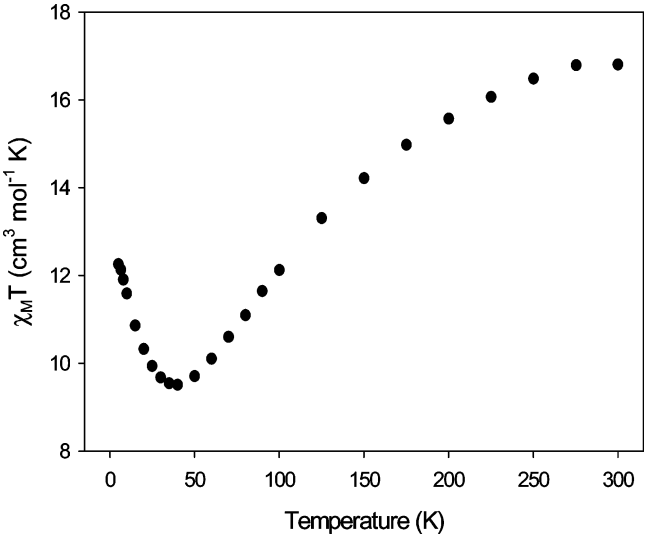

Figure 5. Plot of $\chi_M T$ vs T for complex **1**.

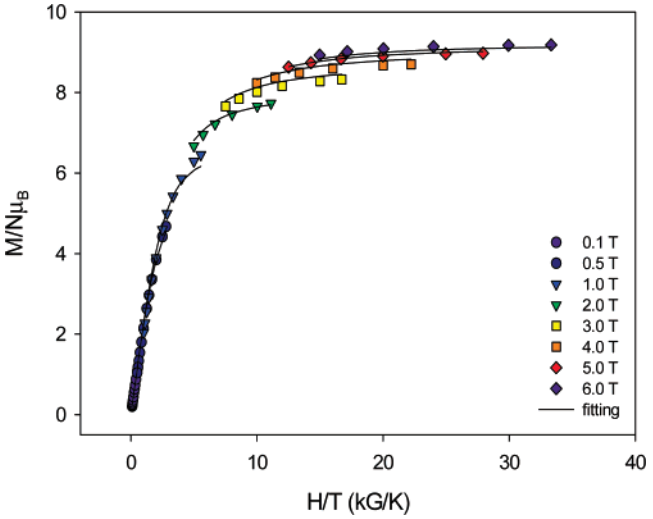

Figure 6. Magnetization (M) vs field (H) and temperature (T) data, plotted as reduced magnetization ($M/N\mu_B$) vs H/T, for complex **1** at applied fields of 0.1−6.0 T and in the 1.8−10 K temperature range. The solid lines are the fit of the data; see the text for the fit parameters.

indicating the presence of dominant antiferromagnetic exchange interactions. The 5.0 K value is consistent with an $S = 5$ ground state, with a g factor slightly less than 2.0, as expected for a Mn^{II}/Mn^{III} complex; the spin-only value for $S = 5$ is 15.0 cm^3 K mol^{-1}. Given the size and low-symmetry of the Mn_6 cation, and the resulting number of inequivalent exchange constants, it is not possible to apply the Kambe method[46] to determine the individual pairwise Mn_2 exchange interaction parameters, and we concentrated instead on characterizing the ground state spin, S, and the zero-field splitting parameter, D.

To confirm the indicated $S_T = 5$ ground state of complex **1** and to determine the magnitude and sign of D, magnetization (M) versus dc field measurements were made on restrained samples in the magnetic field (H) and temperature ranges 1−60 kG and 1.8−10.0 K, respectively. The resulting data for **1** are shown in Figure 6 as a reduced magnetization ($M/N\mu_B$) versus H/T plot, where M is the magnetization, N is Avogadro's number, and μ_B is the Bohr magneton. The data were fit using the program MAGNET[29] to a model that assumes only that the ground state is populated at these temperatures and magnetic fields, includes isotropic Zeeman interactions and axial zero-field splitting ($D\hat{S}_z^2$), and incorporates a full powder average. The corresponding spin Hamiltonian is given by eq 3, where $\hat{S}_z$ is the easy-axis spin operator, and μ_0 is the vacuum permeability.

$$\mathscr{H} = D\hat{S}_z^2 + g\mu_B\mu_0\hat{S}\cdot H \qquad (3)$$

The last term in eq 3 is the Zeeman energy associated with an applied magnetic field. The best fit is shown as the solid lines in Figure 6 and was obtained with $S = 5$, $g = 1.84$, and $D = -0.24$ cm^{-1}. Alternative fits with $S = 4$ or 6 were rejected because they gave unreasonable values of g and D.

As we have described before on multiple occasions,[11a,30,47] ac susceptibility studies are a powerful complement to dc studies for determining the ground state of a system, because they preclude any complications arising from the presence of a dc field. We thus chose to carry out ac studies on complex **1** as an independent determination of its ground state S. These were performed in the 1.8−15 K range using a 3.5 G ac field oscillating at frequencies in the 50−1000 Hz range. If the magnetization vector can relax fast enough to keep up with the oscillating field, then there is no imaginary (out-of-phase) susceptibility signal (χ''_M), and the real (in-phase) susceptibility (χ'_M) is equal to the dc susceptibility. However, if the barrier to magnetization relaxation is significant compared to thermal energy (kT), then the in-phase signal decreases and a nonzero, frequency-dependent χ''_M signal appears, which is suggestive of the superparamagnetic-like properties of an SMM. For complex **1**, the in-phase $\chi'_M T$ signal below 15 K increases with decreasing temperature to a plateau in the 3−4 K region, before decreasing at $T < 3$ K (Figure 7). Extrapolation of the plot to 0 K from above 5 K (to avoid the decrease at lower T due to anisotropy, Zeeman effects, weak intermolecular interactions, etc.) gives a value of ~13.5 cm^3 K mol^{-1}. This indicates an $S = 5$ ground state with $g \sim 1.90$, in satisfying agreement with the dc magnetization fit. Note that $S = 4$ and 6 ground states would be expected to give $\chi'_M T$ values of slightly less than 10 and 21 cm^3 K mol^{-1}, respectively, clearly very different from the experimental values. We conclude that complex **1** (and **2**) is confirmed to have an $S = 5$ ground state. Finally, complex **1** did not exhibit an out-of-phase ac magnetic susceptibility signal down to 1.8 K, indicating that it does not exhibit a barrier large enough (vs kT) to show the superparamagnet-like slow relaxation of its magnetization vector; i.e., it is not an SMM. Studies at much lower temperatures would be required to search for what would at best be a tiny relaxation barrier.

(46) Kambe, K. *J. Phys. Soc. Jpn.* **1950**, *5*, 48.

(47) (a) Sañudo, E. C.; Wernsdorfer, W.; Abboud, K. A.; Christou, G. *Inorg. Chem.* **2004**, *43*, 4137. (b) Murugesu, M.; Raftery, J.; Wernsdorfer, W.; Christou, G.; Brechin, E. K. *Inorg. Chem.* **2004**, *43*, 4203. (c) Scott, R. T. W.; Parsons, S.; Murugesu, M.; Wernsdorfer, W.; Christou, G.; Brechin, E. K. *Angew. Chem., Int. Ed.* **2005**, *44*, 6540.

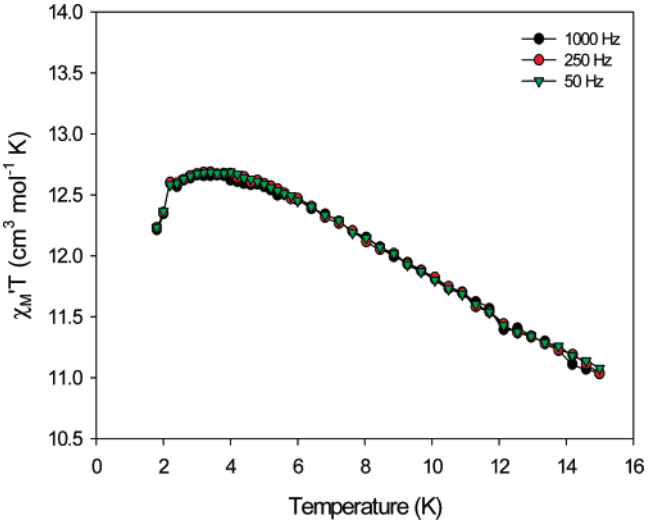

Figure 7. Plot of the in-phase ac susceptibility signals, $\chi'_M T$ vs T for complex **1** at the indicated frequencies.

The $S = 5$ ground state of $2Mn^{II}$, $4Mn^{III}$ complex **1** has not been previously encountered in Mn_6 clusters, and it is distinctly different from the $S = 0$ ground state possessed by the $[Mn_6O_2(O_2CR)_{10}L_4]$ complexes mentioned earlier that also have an edge-sharing bitetrahedral core but a $4Mn^{II}$, $2Mn^{III}$ oxidation state.[38] An $S = 5$ state for a $2Mn^{II}$, $4Mn^{III}$ complex such as **1** that has spin values in the $S = 0-13$ range is consistent with a combination of both ferro- and antiferromagnetic interactions, spin frustration effects within the linked triangular units in a completely antiferromagnetically coupled system, or both. There are thus various possible coupling schemes that could yield an $S = 5$ ground state, making it difficult to rationalize the observed value in a unique manner. Nevertheless, it is expected (i) that the $Mn^{III}\cdots Mn^{III}$ and $Mn^{III}\cdots Mn^{II}$ interactions will be stronger than the $Mn^{II}\cdots Mn^{II}$ one, leaving the latter interaction in the center of the molecule frustrated and the Mn^{II} spins aligned parallel;[48] and (ii) that bridging oximato groups usually give antiferromagnetic interactions,[49,50] although occasionally they give ferromagnetic interactions.[22,51] On the basis of these points, we offer in Figure 8 one spin alignment possibility that would give the observed $S = 5$ ground state of **1**. In this figure, we assume two symmetry-equivalent $Mn^{III}Mn^{II}$ interactions are ferromagnetic, Mn1Mn3 and Mn1′Mn3′; these are bis-monoatomically bridged by an oxide (O7) and a MeO^- (O8M), with corresponding angles of 101.33° and 103.89, respectively, relatively acute values that likely result in ferromagnetic coupling. With all other interactions antiferromagnetic, and the Mn^{II} spins frustrated, as mentioned above, this gives an overall $S = 5$ ground state. Figure 8 offers only one reasonable possibility for how complex **1** has an $S = 5$ ground state; there are, of course, other possibilities.

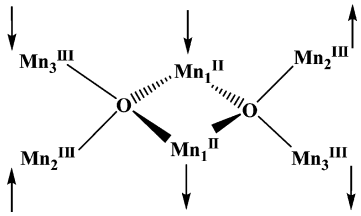

Figure 8. Proposed spin alignments in complex **1** that give the observed $S = 5$ ground state, assuming one type of $Mn^{III}Mn^{II}$ exchange interaction is ferromagnetic, all others are antiferromagnetic, and the $Mn^{II}Mn^{II}$ interaction is completely frustrated. The atom numberings of Figures 1 and 2 are shown as subscripts.

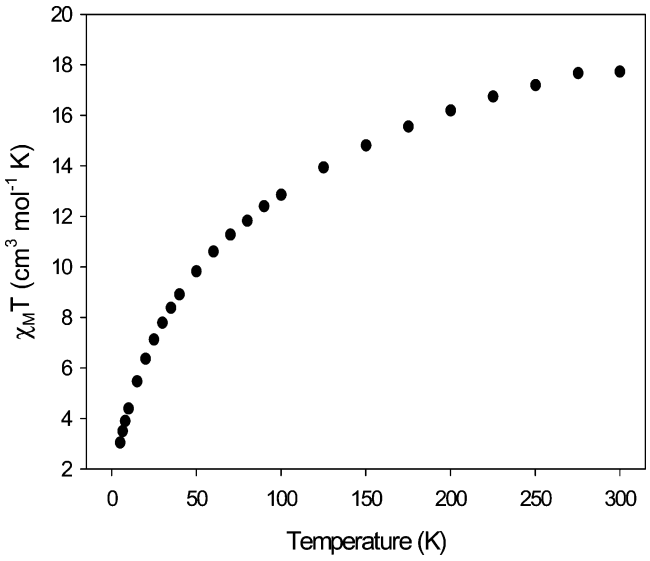

Figure 9. Plot of $\chi_M T$ vs T for complex **3**·$3H_2O$.

Magnetic Susceptibility Studies of Complex 3. Variable-temperature magnetic susceptibility measurements were performed on a microcrystalline powder sample of **3**·$3H_2O$, restrained in eicosane to prevent torquing, in a 1 kG (0.1 T) field and in the 5.0−300 K range. The obtained data are shown as a $\chi_M T$ versus T plot in Figure 9. $\chi_M T$ rapidly decreases from 17.73 cm^3 K mol^{-1} at 300 K to 3.05 cm^3 K mol^{-1} at 5.0 K. Again, the 300 K value is much less than the spin-only ($g = 2$) value of 27.75 cm^3 K mol^{-1} for two Mn^{II} and six Mn^{III} noninteracting ions, indicating the presence of dominant antiferromagnetic exchange interactions and a low, but possibly nonzero, ground state S value. Again, the high nuclearity and low symmetry of the complex make it extremely difficult to evaluate the various exchange parameters. Thus, to determine the ground state of the complex, magnetization data were collected in the magnetic field and temperature ranges 1−60 kG and 1.8−10.0 K. However, we could not get an acceptable fit using data collected over the whole field range, which is a common problem caused by low-lying excited states, especially if some have an S value greater than that of the ground state, as is the case for **3** on the basis of Figure 9. A common solution is to only use data collected with low fields (≤1.0 T), as we previously reported for many mixed-valence Mn^{II}/Mn^{III} clusters.[11a,30,52] However, it was still not possible to obtain a satisfactory fit assuming

(48) Stamatatos, Th. C.; Christou, G. *Phil. Trans. R. Soc. London, Ser. A* **2007**, doi:10.1098/rsta.2007.2144, and references therein.
(49) For a recent review, see: Chaudhuri, P. *Coord. Chem. Rev.* **2003**, *243*, 143.
(50) Pringouri, K. V.; Raptopoulou, C. P.; Escuer, A.; Stamatatos, Th. C. *Inorg. Chim. Acta* **2006**, *360*, 69.
(51) Milios, C. J.; Vinslava, A.; Wernsdorfer, W.; Prescimone, A.; Wood, P. A.; Parsons, S.; Perlepes, S. P.; Christou, G.; Brechin, E. K. *J. Am. Chem. Soc.* **2007**, *129*, 6547 and references therein.

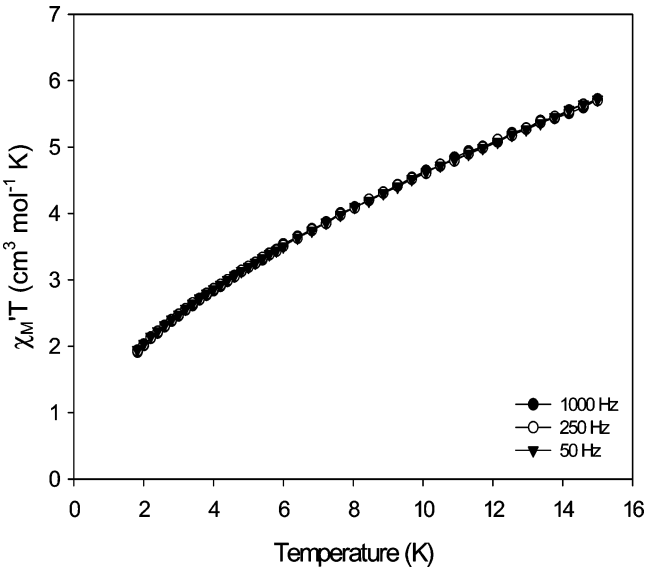

Figure 10. Plot of the in-phase ac susceptibility signals, $\chi_M'T$ vs T for complex **3**·3H_2O at the indicated frequencies.

that only the ground state is populated in this temperature range. This suggests that low-lying excited states are populated, even at these relatively low temperatures. Thus, we turned to ac susceptibility measurements in a 3.5 G ac field oscillating at frequencies in the 50−1000 Hz range. The in-phase χ'_MT versus T data are shown in Figure 10 and show a rapid decrease below 15 K consistent with decreasing population of low-lying excited states with S greater than that of the ground state. The plot does not appear to be heading for $\chi'_MT \sim 0$ at 0 K, and in fact extrapolation of the plot to 0 K gives a χ'_MT value of ~ 1.0 cm^3 K mol^{-1}, which is consistent with an $S = 1$ ground state and $g \sim 2.0$. We cannot rule out the possibility that it is an $S = 0$ ground state with very low-lying $S > 0$ excited states. In any event, complex **3** clearly has a very small ground state spin. As expected, there were no out-of-phase ac signals down to 1.8 K.

Conclusions

We have reported the employment of a new N,N,N,O,O-based pentadentate chelate in transition metal cluster chemistry, one that emphasizes the coordinating ability and versatility of pyridyl oximate-based ligands in coordination chemistry. The resulting anions of 2,6-diacetylpyridine dioxime, dapdoH_2, have been employed in manganese chemistry, and they have provided clean access to three new polynuclear, valence-trapped, Mn(II/III) clusters, **1**−**3**. In particular, the reaction between $[Mn_3O(O_2CMe)_6(py)_3](ClO_4)$ and dapdoH_2 has led to the hexanuclear complex $[Mn_6O_2(OMe)_2(dapdo)_2(dapdoH)_4](ClO_4)_2$ (**1**), whereas the reaction between $Mn(NO_3)_2$, $Ca(NO_3)_2$, and dapdoH_2 in basic media has led to the similar $[Mn_6O_2(OMe)_2(dapdo)_2(dapdoH)_4][Ca(NO_3)_4]$ (**2**) cluster, both possessing the rare "edge-sharing tetrahedron" Mn_6O_2 core. A similar reaction but with the addition of NaN_3 gives the octanuclear cluster $[Mn_8O_4(OH)_4(OMe)_2(N_3)_2(dapdo)_2(dapdoH)_2(H_2O)]$ (**3**) with an interesting core described as two oxo-linked $[Mn^{II}Mn^{III}_3(\mu_3\text{-}O)_2]^{7+}$ "butterfly" units. It is also interesting that the azide ligands in **3** are terminal rather than bridging but, nevertheless, fostered formation of a product completely different from that of the non-azide products **1** and **2**. As a result of the coordination characteristics of dapdo$^{-/2-}$ ligands, complexes **1** and **2** have significant ground state spin values of $S = 5$, while for complex **3** the exact determination of the ground state spin value is currently unfeasible due to its complicated structure and presence of spin frustration effects. It will be interesting to determine, as this work is extended, to what extent dapdo$^{-/2-}$ will continue to provide a route to new metal clusters and to what extent these are related to clusters provided by pyridyl monooximes (mpko$^-$) and pyridyl alcohols (pdm$^{-/2-}$) alone.

Note Added in Proof: After submission of this paper, the heterometallic complex $[Cu_2Cr_2(OH)_2Br_2(dapdo)_2(tacn)_2]^{2+}$ was reported. See: Khanra, S.; Weyhermüller, T.; Chaudhuri, P. *Dalton Trans.* **2007**, 4675.

Acknowledgment. This work was supported by the NSF (CHE-0414555 to G.C.).

Supporting Information Available: X-ray crystallographic files in CIF format for complexes **1**·H_2O, **2**·*x*(solvents), and **3**·*x*H_2O. This material is available free of charge via the Internet at http://pubs.acs.org.

IC7020269

(52) (a) King, P.; Wernsdorfer, W.; Abboud, K. A.; Christou. G. *Inorg. Chem.* **2005**, *44*, 8659. (b) Tasiopoulos, A. J.; Wernsdorfer, W.; Abboud, K. A.; Christou, G. *Inorg. Chem.* **2005**, *44*, 6324.